ACS Macro Letters

Letter

pubs.acs.org/macroletters

An Approach for the Sphere-to-Rod Transition of Multiblock Copolymer Micelles

Hong Tan,* Zhigao Wang, Jiehua Li, Zhicheng Pan, Mingming Ding, and Qiang Fu

College of Polymer Science and Engineering, State Key Laboratory of Polymer Materials Engineering, Sichuan University, Chengdu 610065, China

Supporting Information

ABSTRACT: The shape of polymer micelles is important for pharmaceutical applications as drug delivery. In this article, an approach inducing sphere-to-rod transition of multiblock polyurethane micelles has been developed through introducing a second hydrophilic component phosphatidylcholine group into the polymer chains. Time-resolved dynamic light scattering (DLS), combined with transmission electron microscopy (TEM), was employed to investigate the kinetics of morphology transition. Moreover, a dissipative particle dynamics (DPD) simulation method was applied to study the mechanism of sphere-to-rod transition. These experimental and simulation studies revealed that the hydrophilic phosphatidylcholine groups can create defects on the surfaces of spherical polyurethane micelles, thus, making positive contribution to adhesive collisions and leading to the fusion of spherical micelles into rod-like micelles. This finding provides new insight into the origins of rod-like polymer micelles, which is valuable for the design and preparation of novel polymeric drug carriers with tailored properties.

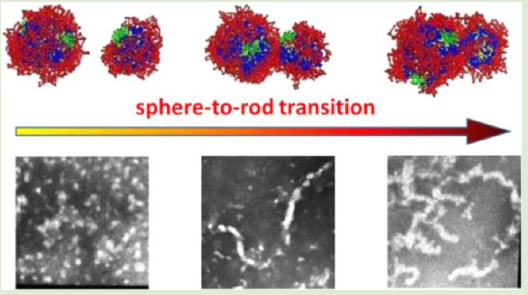

It is well-known that amphiphilic block copolymers can self-assemble into nanoscopic core−shell micelles in aqueous solutions. The hydrophobic blocks of the copolymer are segregated to form the inner core that can encapsulate poorly water-soluble drugs, and the hydrophilic blocks form the corona or outer shell that makes the micelle water-soluble. Therefore, polymeric micelles have long been well recognized as excellent candidates for drug delivery carriers.[1−6] In particular, diblock and triblock copolymers, mainly based on polyethylene glycol (PEG) and polylactide (PLA) or polycaprolactone (PCL), have been extensively investigated for their unique micelle structures in therapeutic and diagnostic applications in the past decades.[7−9] These polymeric micelles can give rise to a variety of aggregate structures, such as spherical micelles, ellipsoidal micelles, rod-like micelles (worm-like micelles), disc-like micelles, vesicles, and large compound micelles.[10−12] Among them, rod-like micelles become more attractive due to their high drug loading content,[13] high surface area for controlled release,[14] prolonging circulation times in vivo,[15] and easy internalization into tumor cells.[16,17] As a result, great efforts have been devoted to studying the formation of rod-like micelles.[13−17] Generally, the rod-like micelles of diblock and triblock copolymers can be obtained from their sphere micelles by varying such factors as the block length, polydispersity and molecular curvature of the copolymer,[18] initial polymer concentration,[19] temperature,[20] the solvent composition,[21] the presence of additives (salt, acid, homopolymer),[22−24] solvent addition rate,[25] crystalline nature of the core-forming blocks,[26] and so on. These factors play dominant roles in changing the elastic free energy of the cores or generating some defects on their surfaces.[27] The aggregate morphologies of block copolymers are controlled by a balance of three contributions to the free energy of the system, the stretching of the core-forming blocks, the repulsive interaction among the corona chains, and the surface tension between the micelle cores, which have been intensively investigated by Eisenberg and co-workers.[28−31]

On the other hand, several researchers have been attracted to developing multiblock copolymer micelles for antitumor drug delivery that could conquer the shortages of diblock and triblock copolymer micelles such as limited encapsulation, initial burst, single function, and lack of control over both micellization and drug delivery properties.[32−34] In comparison with traditional copolymers, these multiblock copolymers can endow with more control over polymer self-assembly, enlarge the structure diversity, and allow access to multicompartment micelles and incorporation of extra functionality.[35,36] Recently, strongly motivated by these virtues of multiblock copolymers, research in our group has been focused on the development of biodegradable multiblock polyurethane micelles with various structures and functionalities for drug delivery and bioimaging applications,[37−43] because biodegradable multiblock polyurethanes possess good biocompatibility, excellent molecular tailorability, and feasibility of incorporating functional moieties.[41] For example, gemini quaternary ammonium (GQA) pendant groups used as cell internalization promoters were effortlessly introduced into the polyurethane side chains with

Received: October 21, 2012
Accepted: January 18, 2013
Published: January 25, 2013

   dx.doi.org/10.1021/mz3005583 | ACS Macro Lett. 2013, 2, 146−151

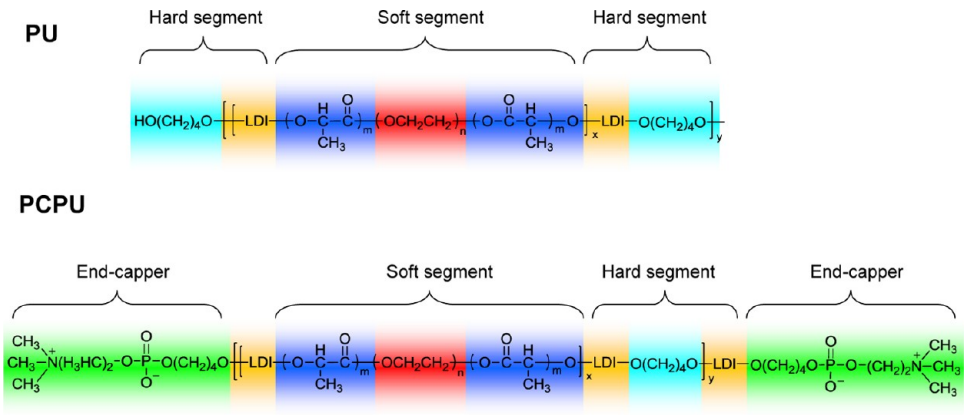

Figure 1. Structures of nonphosphatidylcholine polyurethane (PU) and phosphatidylcholine-capped polyurethane (PCPU).

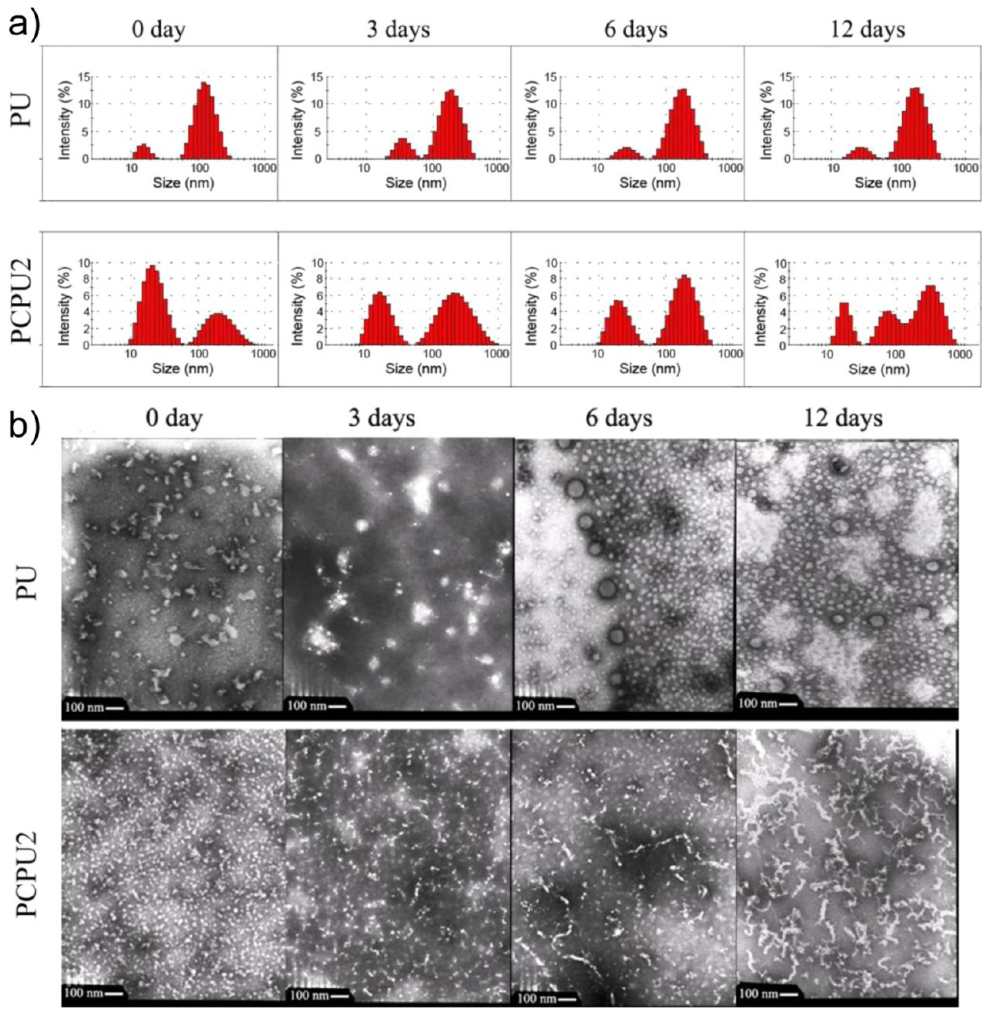

Figure 2. Size distributions (a) and TEM images (b) of PU and PCPU2 micelles after 0, 3, 6, and 12 days of storage. The bars are 100 nm. The initial concentration was 1.0 mg/mL.

controlled charge density, and methoxy polyethylene glycol (mPEG) end-capped the polymer chains played a key role in further regulating the cationic intensity of carriers and providing good protection of these positive polymers from the reticuloendothelial system (RES).[39,40] Phosphatidylcholine group end-capped polyurethane chains provide biomimetic structure to improve the biocompatibility, tumor cell uptake,[44] and micellization characteristics.[42] Interestingly, we discovered that some rod-like polyurethane micelles could be easily obtained without complicated controlling conditions in the multiblock polyurethane systems containing two or more different hydrophilic blocks. To the best of our knowledge, few efforts have yet been made to explore the mechanism of rod-like micelle formation of multiblock polymers.

In this paper, using phosphatidylcholine end-capped polyurethanes as an example, sphere-to-rod transition of the

dx.doi.org/10.1021/mz3005583 | ACS Macro Lett. 2013, 2, 146−151

polyurethane micelles in aqueous solutions was directly observed by dynamic light scattering (DLS) and transmission electron microscopy (TEM). Dissipative particle dynamics (DPD) simulation, a mesoscopic simulation method for complex fluids originally developed by Hoogerbrugge and Koelman,[45,46] was employed in an attempt to explain the mechanism of morphological transition. Additionally, drug loading experiments were performed to confirm the benefits of sphere-to-rod transition.

The phosphatidylcholine-capped polyurethanes previously synthesized in our laboratory were employed in this study.[42] The structures of these polymers are illustrated in Figure 1. The polyurethane samples are denoted as PCPU1, PCPU2, and PCPU3, of which the theoretical molar fraction of phosphatidylcholine is 4.88, 9.52, and 13.95%, respectively. Also, polyurethane without phosphatidylcholine groups as a blank is denoted as PU.

Polyurethane micelles were prepared by a dialysis method (Supporting Information). It has been demonstrated that the shape of drug delivery particles plays a key role in therapeutic applications.[11] Herein, the process of spherical-to-rod transition of multiblock polyurethane micelles is disclosed. DLS was first applied to detect the changes in size distributions of the micelles over time. Figure 2a shows the hydrodynamic diameter (D_h) distributions of PU and PCPU2 micelles after 0, 3, 6, and 12 days of storage. Bimodal distribution was observed for PU micelles, and the primary micelles with D_h peaked at 20 nm coexisted with the micellar aggregates peaked at 100 nm in the beginning. Furthermore, their sizes and area ratios almost did not change over a 12 day storage. For phosphatidylcholine-capped polyurethane micelles, taking PCPU2 as an example, bimodal size distribution was also observed at the beginning. However, the amount of the primary micelles around 20 nm was more than that around 100 nm in diameter. After 3 days of storage, the number of the micelles around 100 nm increased, and the primary micelle number correspondingly decreased. At day 6, the transition trend still remained, and the size distribution was slightly narrowed. As the storage time increased to 12 days, there was a trimodal size distribution of PCPU2 micelles. Apparently, a new peak at 80 nm appeared between the two peaks at 20 and 300 nm owing to the existence of three components in the system, including primary micelles, micelle aggregates, and newly formed aggregates. These results indicated that an increasing number of unassociated primary micelles were incorporated into the micellar aggregates for phosphatidylcholine-capped polyurethanes.

To further understand the aggregation behavior of phosphatidylcholine-capped polyurethane micelles, the size variation of these micelles with time evolution was plotted in Figure S1. It was found that all phosphatidylcholine-capped polyurethane micelles had low initial sizes and their diameters increased sharply over time. More phosphatidylcholine content in these polyurethanes is favorable for a faster increase in size. Taking PCPU2 micelle as an example, a 2.7-fold increase of micellar size (from 30 to 80 nm) was attained with time evolution. Contrarily, a minor increase of 20% in the average diameter was observed for PU micelles without phosphatidylcholine in 12 days of storage, suggesting that hydrophilic phosphatidylcholine groups contribute significantly to the merging of polyurethane micelles.

To directly observe the aggregation process of phosphatidylcholine-capped polyurethane micelles, TEM was employed to determine the morphologies of these micelles at different time. Figure 2b displays the morphologies of PCPU2 and PU micelles obtained by TEM after 0, 3, 6, and 12 days of storage. It was observed that the PU sample first forms irregular micelles of different sizes, and then gradually reorganizes into spherical micelles with sizes ranging from around 20 to 100 nm over time. The sizes of these spherical micelles remain unchanged from 6 to 12 days of storage, suggesting that the micelle system has reached a steady state without further merging of spherical micelles into rod-like micelles. It should be noted that all the average diameters of micelles observed by TEM are smaller than those determined by DLS, because the samples for TEM observations were dried micelles after solvent evaporation.[47] In contrast, the aggregation of phosphatidylcholine-capped polyurethane micelles could spontaneously occur in storage (Figure 2b). At the beginning, the PCPU2 chains mainly self-assemble into small spherical micelles with an average diameter of 20 nm. After 3 days, most of the spheres have merged to form irregular "pearl necklace" structures. With time evolution, the connection of micelles continuously occur, and the pearl necklace intermediates eventually reorganize to form rod-like micelles to reduce the surface area of the aggregates. As a result, a mixture of spherical micelles and rod-like micelles was observed after 6 days of storage. After 12 days, most spherical micelles have assembled into rod-like micelles, and small rod-like micelles could further aggregate into larger ones or worm-like micelles. The result is in good agreement with the DLS measurement results for PCPU2, indicating that there were three components (primary micelles, rod-like micelles, and newly formed worm-like micelles) in the system. Apparently, the growth of rod-like micelles was a spontaneous process without any regulation. Nevertheless, it was found that the size of micelles remained unchanged and the whole micellar solution was stable over a period of months. A possible explanation is that the free energy of rod-like micelles would be increased by further increase of aggregation number, which is thermodynamically unfavorable.[31,48] In addition, there are also some thick micelles with larger size in second dimension after 12 days (Figure 2b). This may be resulted from the overlay of dried micelles. However, the further aggregation of rod- or worm-like micelles should also be taken into account. More work is needed to better understand this phenomenon.

As described above, the phosphatidylcholine-capped polyurethane micelles could undergo a sphere-to-rod transition, while polyurethane only containing hydrophilic PEG blocks forms spherical micelles. This indicates that the phosphatidylcholine group plays a key role in the sphere-to-rod transition of polyurethane micelles. Similarly, we have previously found that the incorporation of a second hydrophilic GQA component into PEG-based multiblock polyurethanes can lead to the formation of rod-like or worm-like micellar structures.[40] In another work, we have also demonstrated that when the monoclonal antibody was covalently attached onto the surface of polyurethane micelles, the micellar morphology was transformed from spheres to cylinders.[43] It is believed that the morphology transition is not only caused by the unique molecular structure of multiblock polyurethanes, but also because the additional hydrophilic components incorporated disturb the force balance governing the aggregation structures.[31,49] Therefore, it is valuable to disclose the mechanism that phosphatidylcholine groups capped onto polyurethane chain ends can give impetus to sphere-to-rod transition of these

dx.doi.org/10.1021/mz3005583 | ACS Macro Lett. 2013, 2, 146−151

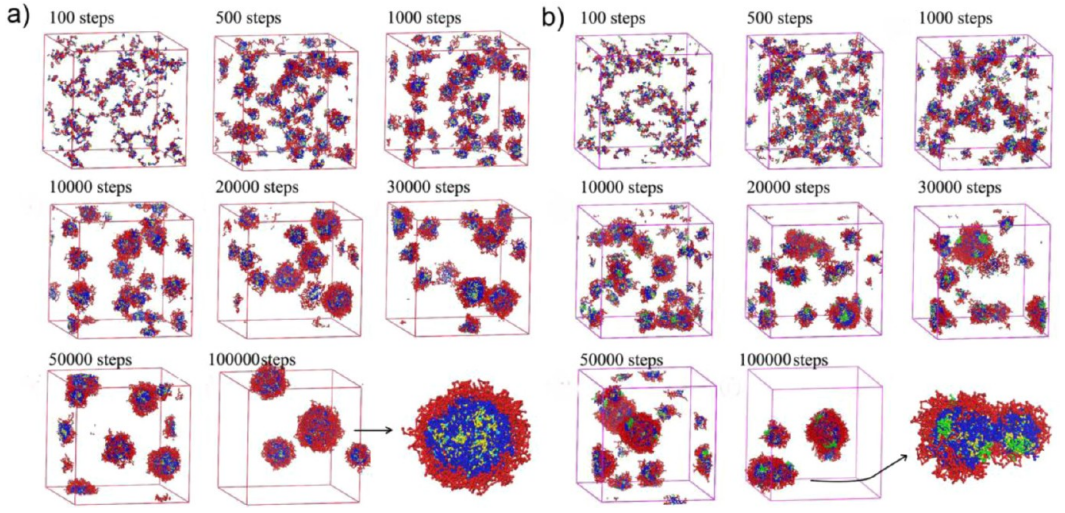

Figure 3. Micellar aggregation morphologies of (a) PU and (b) PCPU2 at 5% concentration with increasing simulation steps. The insets show enlarged section views of micelles after 100000 step simulations. PLA, PEG, BPC, LDI, and BDO segments are represented by blue, red, green, yellow, and cyan, respectively. To observe the aggregation behavior clearly, the water beads were not shown.

polyurethane micelles. This will provide a novel avenue for facile preparation of rod-like polymer micelles.

However, due to the small size of micelles, the aggregation process of spherical micelle into rod-like ones can be hardly observed from TEM images. Therefore, DPD simulation, a powerful tool to study the morphologies of multicompartment micelles formed from multiblock polymers in water,[40,50−53] was performed to provide more evidence of micelle aggregation. As shown in Figure 3, PCPU2 molecules are disordered in aqueous solution at the beginning (100 simulation steps). With the step increased to 500 and 1000, the polymer molecules begin to aggregate and form small micelles of various sizes, because these lipophilic PLA blocks have the trend of spontaneous aggregation in the aqueous medium.[54] Aggregations of PLA gradually transform into spheres under the action of surface tension, while hydrophilic PEG blocks get wrapped on the surface progressively. As simulation progressed, more and more micelles tend to aggregate together with size increasing and number decreasing, and both spherical and rod-like micelles are observed in the figures. Finally, only one big spherical micelle and two rod-like micelles could be found, and PEG and BPC were wrapped on the surfaces. By contrast, the simulation results of PU present four spherical micelles at 100000 simulation steps, without any rod-like assemblies formed during the simulation process (Figure 3a). These results suggest that PCPU micelles containing phosphatidylcholine groups hold greater potential to undergo a sphere-to-rod transition compared to PU micelles, which is in good agreement with DLS and TEM measurements.

To study the kinetics of the sphere-to-rod transition, we monitored the morphology transition of PCPU2 micelles via both simulation and TEM. As seen from Figure 4, there are two spherical micelles with PEG shell and several globs of phosphatidylcholine aggregated on the surfaces at the beginning. With time evolution, the two spheres get close, and their PEG chains begin to intertwine with each other. PEG on the surfaces and PLA in the cores continue to integrate, and finally they fuse into a rod-like micelle. The simulation results were consistent with the TEM images (Figure 4). Thus, the sphere-to-rod transition of multiblock polyurethanes should be attributed to the polar phosphatidylcholine groups self-

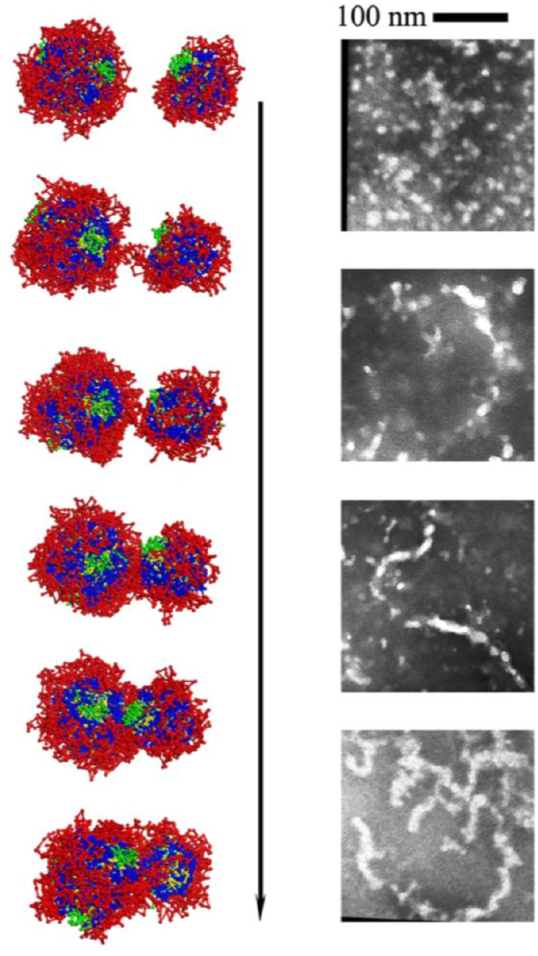

Figure 4. Sphere-to-rod transition of PCPU2 micelles observed via simulation and TEM. The bar is 100 nm.

assembling onto the micelle surfaces excluded the PEG shell, resulting in some defects on the micelle surfaces. The defects lead to the exposure of PLA core chains onto the micelle surfaces, which attracts to each other due to the interface instabilities of sphere micelles.[27] Eventually, sphere-to-rod

dx.doi.org/10.1021/mz3005583 | ACS Macro Lett. 2013, 2, 146−151

transition occurs gradually. This phenomenon might also be explained by Eisenberg's theory.[31,49] Exposed PLA core leads to an increase in the stretching of the core-forming blocks, and the repulsive interaction among the shell chains of different micelles is reduced due to the defects on the PEG shell. Therefore, the spherical micelles undergo adhesive collisions to form rod-like micelles. This finding provides new understanding on the formation of rod-like polymer micelles, which is valuable for the design and preparation of novel polymeric drug carriers with tailored properties. Further work is being carried out to apply this concept to other multiblock copolymer systems.

It is well-recognized that rod-like micelles have shown improved pharmacological effects compared to their spherical counterparts.[43,55] Herein, to verify the impact of morphology transition on the drug loading capacity of multiblock polyurethane micelles, the amount of antitumor drug PTX loaded into different polyurethane micelles was illustrated in Figure S2. It was found that PU micelle had a low drug loading content of 4% with 7% encapsulation efficiency, while PCPU micelles exhibited higher encapsulation capacity, of which drug loading content and encapsulation efficiency were markedly increased with phosphatidylcholine incorporation. Particularly, the highest loading content and encapsulation efficiency of 10.97% and 50% were obtained for PCPU2 micelles, respectively. These results are similar to those obtained in our earlier work, where an improved drug loading content was found for antibody-conjugated cylindrical micelles.[43] Such an increase of drug loading capacity is probably due to that the formation of rod-like micelles can provide a larger core volume for the encapsulation of therapeutic agents.[56] In addition, it has been shown that rod-like nanoparticles exhibit much more rapid and efficient cell internalization, prolonged blood circulation, and higher tumor uptake, as well as enhanced and sustained antitumor effects compared to their spherical counterparts.[17,57] While several other reports have instead found that spherical nanocarriers were internalized to a greater extent than their corresponding rod-shaped or cylindrical particles.[58] In view of these controversial findings, the careful design and fabrication of rod-like micelles with controlled length and dispersity is clearly needed to optimize the nanocarrier platforms for in vivo therapeutic applications. Fortunately, the group of Winnik has recently developed a crystallization-driven living self-assembly strategy to obtain cylindrical micelles with precisely controlled length and architecture.[59] In our work, the structure and content of the additional hydrophilic component can be tuned to change the interface instability and the defect on micellar surface and, thus, to provide more control over the sphere-to-rod transition.

In summary, the process of spherical-to-rod transition for multiblock polyurethane micelles containing two different hydrophilic components PEG and phosphatidylcholine groups has been directly disclosed using DSL and TEM. The mechanism of morphology transition is ascribed to the defects on the sphere micelle surfaces generated by the second hydrophilic component phosphatidylcholine groups, which cause the fusion of sphere micelles into rod-like micelles, as demonstrated by DPD simulation. The sphere-to-rod transition can moderately increase the drug loading capacity of polyurethane micelles. Therefore, our research is of great significance in the control of micelle agglomeration and the preparation of assemblies with desirable properties by molecular design. Further works are currently being carried out in our group to investigate the internalization of rod-like polyurethane micelles by tumor cells.

■ ASSOCIATED CONTENT

Supporting Information

Materials, instrumentation, experimental conditions, and additional results. This material is available free of charge via the Internet at http://pubs.acs.org.

■ AUTHOR INFORMATION

Corresponding Author

*E-mail: hongtan@scu.edu.cn.

Notes

The authors declare no competing financial interest.

■ ACKNOWLEDGMENTS

We express our great thanks to the National Natural Science Foundation of China (51073104 and 51173118), Changjiang Scholars and Innovative Research Team in University (IRT1163), and the Sichuan Provincial Science Fund for Distinguished Young Scholars (09ZQ026-024) for financial support. The authors would also like to thank Prof. Shaobing Zhou at Key Laboratory of Advanced Technologies of Materials, Ministry of Education, Southwest Jiaotong University of China, for DLS measurements.

■ REFERENCES

(1) Kwon, G. S.; Okano, T. *Adv. Drug Delivery Rev.* **1996**, *21*, 107–116.
(2) Kataoka, K.; Harada, A.; Nagasaki, Y. *Adv. Drug Delivery Rev.* **2001**, *47*, 113–131.
(3) Haag, R. *Angew. Chem., Int. Ed.* **2004**, *43*, 278–282.
(4) Nasongkla, N.; Bey, E.; Ren, J. M.; Ai, H.; Khemtong, C.; Guthi, J. S.; Chin, S. F.; Sherry, A. D.; Boothman, D. A; Gao, J. M. *Nano Lett.* **2006**, *6*, 2427–2430.
(5) Torchilin, V. P. *Pharm. Res.* **2007**, *24*, 1–16.
(6) Park, J. H.; Lee, S.; Kim, J. H.; Park, K.; Kim, K.; Kwon, I. C. *Prog. Polym. Sci.* **2008**, *33*, 113–137.
(7) Lavasanifar, A.; Samuela, J.; Kwon, G. S. *Adv. Drug Delivery Rev.* **2002**, *54*, 169–190.
(8) Agrawal, S. K.; Sanabria-DeLong, N.; Coburn, J. M.; Tew, G. N.; Bhatia, S. R. *J. Controlled Release* **2006**, *112*, 64–71.
(9) Lu, J.; Ma, S. L.; Sun, J. Y.; Xia, C. C.; Liu, C.; Wang, Z. Y.; Zhao, X. N.; Gao, F. B.; Gong, Q. Y.; Song, B.; Shuai, X. T.; Ai, H.; Gu, Z. W. *Biomaterials* **2009**, *30*, 2919–2928.
(10) Buchnall, D. G.; Anderson, H. L. *Science* **2003**, *302*, 1904–1905.
(11) Venkataraman, S.; Hedrick, J. L.; Ong, Z. Y.; Yang, C.; Ee, P. L. R.; Hammond, P. T.; Yang, Y. Y. *Adv. Drug Delivery Rev.* **2011**, *63*, 1228–1246.
(12) Holder, S. J.; Sommerdijk, N. A. J. M. *Polym. Chem.* **2011**, *2*, 1018–1028.
(13) Tan, J. P. K.; Kim, S. H.; Nederberg, F.; Appel, E. A.; Waymouth, R. M.; Zhang, Y. *Small* **2009**, *5*, 1504–1507.
(14) Kraitzer, A.; Ofek, L.; Schreiber, R.; Zilberman, M. *J. Controlled Release* **2008**, *126*, 139.
(15) Doshi, N.; Mitragotri, S. *Adv. Funct. Mater.* **2009**, *19*, 3843–3854.
(16) Yang, K.; Ma, Y. Q. *Nat. Nanotechnol.* **2010**, *5*, 579–583.
(17) Gratton, S. E. A.; Ropp, P. A.; Pohlhaus, P. D.; Luft, J. C.; Madden, V. J.; Napier, M. E.; DeSimone, J. M. *Proc. Natl. Acad. Sci. U.S.A.* **2008**, *105*, 11613–11618.
(18) (a) Azzam, T.; Eisenberg, A. *Angew. Chem., Int. Ed.* **2006**, *45*, 7443–7447. (b) Schmitt, A. L.; Repollet-Pedrosa, M. H.; Mahanthappa, M. K. *ACS Macro Lett.* **2012**, *1*, 300–304.
(19) Tung, P. H.; Kuo, S. W.; Chen, S. C.; Lin, C. L.; Chang, F. C. *Polymer* **2007**, *48*, 3192–3200.

(20) Bhargava, P.; Tu, Y. F.; Zheng, J. X.; Xiong, H. M.; Quirk, R. P.; Cheng, S. Z. D. *J. Am. Chem. Soc.* **2007**, *129*, 1113−1121.
(21) Yu, Y.; Zhang, L.; Eisenberg, A. *Macromolecules* **1998**, *31*, 1144−1154.
(22) Zhang, L.; Eisenberg, A. *Macromolecules* **1996**, *29*, 8805−8815.
(23) Tyler, C. A.; Morse, D. C. *Macromolecules* **2003**, *36*, 3764−3774.
(24) Matsen, M. W.; Schick, W. *Macromolecules* **1994**, *27*, 7157−7163.
(25) Han, Y. Y.; Yu, H. Z.; Du, H. B.; Jiang, W. *J. Am. Chem. Soc.* **2010**, *132*, 1144−1150.
(26) (a) Massey, J. A.; Temple, K.; Cao, L.; Rharbi, Y.; Raez, J.; Winnik, M. A.; Manners, I. *J. Am. Chem. Soc.* **2000**, *122*, 11577−11584. (b) Rupar, P. A.; Chabanne, L.; Winnik, M. A.; Manners, I. *Science* **2012**, *337*, 559−562.
(27) Zhulina, E. B.; Adam, M.; LaRue, I.; Sheiko, S. S.; Rubinstein, M. *Macromolecules* **2005**, *38*, 5330−5351.
(28) Shen, H.; Zhang, L.; Eisenberg, A. *J. Phys. Chem. B* **1997**, *24*, 4697−4708.
(29) Zhang, L.; Eisenberg, A. *Macromolecules* **1999**, *32*, 2239−2249.
(30) Shen, H.; Eisenberg, A. *Macromolecules* **2000**, *33*, 2561−2572.
(31) Burker, S. E.; Eisenberg, A. *Langmuir* **2001**, *17*, 6705−6714.
(32) Schmidt, V.; Giacomelli, C.; Lecolley, F.; Lai-Kee-Him, J.; Brisson, A. R.; Borsali, R. *J. Am. Chem. Soc.* **2006**, *128*, 9010−9011.
(33) Zhang, X. W.; Ke, F. Y.; Han, J.; Ye, L.; Liang, D. H.; Zhang, A. Y.; Feng, Z. G. *Soft Matter* **2009**, *5*, 4797−4803.
(34) Zou, T.; Li, S. L.; Zhang, X. J.; Wu, S. X.; Cheng, S. X.; Zhuo, R. X. *J. Polym. Sci., Part A: Polym. Chem.* **2007**, *45*, 5256−5265.
(35) Ludwigs, S.; Boker, A.; Voronov, A.; Rehse, N.; Magerle, R.; Krausch, G. *Nat. Mater.* **2003**, *2*, 744−747.
(36) Ott, C.; Hoogenboom, R.; Hoeppener, S.; Wouters, D.; Gohy, J. F.; Schubert, U. S. *Soft Matter* **2009**, *5*, 84−91.
(37) (a) Wang, Z. G.; Yu, L. Q.; Ding, M. M..; Tan, H.; Li, J. H.; Fu, Q. *Polym. Chem.* **2011**, *2*, 601−607. (b) Yu, L. Q.; Zhou, L. J.; Ding, M. M.; Li, J. H.; Tan, H.; Fu, Q.; He, X. L. *J. Colloid Interface Sci.* **2011**, *358*, 376−383. (c) Zhou, L. J.; Liang, D.; He, X. L.; Li, J. H.; Tan, H.; Li, J. S.; Fu, Q.; Qun, Gu. *Biomaterials* **2012**, *33*, 2734−2745.
(38) (a) Ding, M. M.; Li, J. H.; Fu, X. T.; Zhou, J.; Tan, H.; Gu, Q.; Fu, Q. *Biomacromolecules* **2009**, *10*, 2857−2865. (b) Ding, M. M.; Qian, Z. Z.; Wang, J.; Li, J. H.; Tan, H.; Gu, Q.; Fu, Q. *Polym. Chem.* **2011**, *2*, 885−891.
(39) (a) Ding, M. M.; Zhou, L. J.; Fu, X. T.; Tan, H.; Li, J. H.; Fu, Q. *Soft Matter* **2010**, *6*, 2087−2092. (b) Ding, M. M.; He, X. L.; Zhou, L. J.; Li, J. H.; Tan, H.; Fu, X. T.; Fu, Q. *J. Controlled Release* **2011**, *152*, e87−e89.
(40) Ding, M. M.; He, X. L.; Wang, Z. G.; Li, J. H.; Tan, H.; Deng, H.; Fu, Q.; Gu, Q. *Biomaterials* **2011**, *32*, 9515−9524.
(41) Ding, M. M.; Li, J. H.; Tan, H.; Fu, Q. *Soft Matter* **2012**, *8*, 5414−5428.
(42) Wang, Z. G.; Wan, P. J.; Ding, M. M.; Yi, X.; Li, J. H.; Fu, Q.; Tan, H. *J. Polym. Sci., Part A: Polym. Chem.* **2011**, *49*, 2033−2042.
(43) Ding, M. M.; Li, J. H.; He, X.; Song, N. J.; Tan, H.; Zhang, Y.; Zhou, L.; Gu, Q.; Deng, H.; Fu, Q. *Adv. Mater.* **2012**, *24* (27), 3639−3645.
(44) Tu, S.; Chen, Y. W.; Qiu, Y. B.; Zhu, K.; Luo, X. L. *Macromol. Biosci.* **2011**, *11*, 1416−1425.
(45) Hoogerbrugge, P. J.; Koelman, J. *Europhys. Lett.* **1992**, *19*, 155−160.
(46) Koelman, J.; Hoogerbrugge, P. J. *Europhys. Lett.* **1993**, *21*, 363−368.
(47) Giacomelli, C.; Le, M. L.; Borsali, R.; Lai-Kee-Him, J.; Brisson, A.; Armes, S. P.; Lewis, A. L. *Biomacromolecules* **2006**, *7*, 817−828.
(48) Ikeda, S. *J. Phys. Chem.* **1984**, *88*, 2144−2149.
(49) Zhang, L.; Eisenberg, A. *J. Am. Chem. Soc.* **1996**, *118*, 3168−3181.
(50) (a) Wang, Z. G.; Li, J. H.; Tan, H.; Zhang, X. Q.; Fu, Q. *Mol. Simul.* **2009**, *35*, 638−647. (b) Wang, Z. G.; Chen, Y. W.; Li, J. H.; Luo, X. L.; Tan, H. *J. Comput. Theor. Nanosci.* **2011**, *8*, 1910−1915. (c) Li, J. H.; Chen, Y. Z.; Wang, Z. G.; Ding, M. M.; Tan, H.; Fu, Q.; Jiang, X. *Langmuir* **2011**, *27*, 10859−10866.
(51) Xia, J.; Zhong, C. L. *Macromol. Rapid Commun.* **2006**, *27*, 1654−1659.
(52) Zhong, C. L.; Liu, D. H. *Macromol. Theory Simul.* **2007**, *16*, 141−157.
(53) Huang, C. I.; Liao, C. H.; Lodge, T. P. *Soft Matter* **2011**, *7*, 5638−5647.
(54) Guo, X. D.; Zhang, L. J.; Qian, Y.; Zhou, J. *Chem. Eng. J.* **2007**, *131*, 195−201.
(55) Shuvaev, V. V.; Ilies, M. A.; Simone, E.; Zaitsev, S.; Kim, Y.; Cai, S.; Mahmud, A.; Dziubla, T.; Muro, S.; Discher, D. E.; Muzykantov, V. R. *ACS Nano* **2011**, *5*, 6991−6999.
(56) Geng, Y.; Discher, D. E. *J. Am. Chem. Soc.* **2005**, *127*, 12780−12781.
(57) (a) Geng, Y.; Dalhaimer, P.; Cai, S.; Tsai, R.; Tewari, M.; Minko, T.; Discher, D. E. *Nat. Nanotechnol.* **2007**, *2*, 249−255. (b) Christian, D. A.; Cai, S.; Garbuzenko, O. B.; Harada, T.; Zajac, A. L.; Minko, T.; Discher, D. E. *Mol. Pharmaceutics* **2009**, *6*, 1343−1352. (c) Park, J.; von Maltzahn, G.; Zhang, L.; Schwartz, M. P.; Ruoslahti, E.; Bhatia, S. N.; Sailor, M. J. *Adv. Mater.* **2008**, *20*, 1630−1635.
(58) (a) Zhang, K.; Fang, H.; Chen, Z.; Taylor, J. A.; Wooley, K. L. *Bioconjugate Chem.* **2008**, *19*, 1880−1887. (b) Chen, T.; Guo, X.; Liu, X.; Shi, S.; Wang, J.; Shi, C.; Qian, Z.; Zhou, S. *Adv. Healthcare Mater.* **2012**, *1*, 214−224.
(59) (a) Wang, X.; Guerin, G.; Wang, H.; Wang, Y.; Manners, I.; Winnik, M. A. *Science* **2007**, *317*, 644−647. (b) Gilroy, J. B.; Gadt, T.; Whittell, G. R.; Chabanne, L.; Mitchels, J. M.; Richardson, R. M.; Winnik, M. A.; Manners, I. *Nat. Chem.* **2010**, *2*, 566−570.